



**Development of a Procedure to Apply
Leak-Before-Rupture Concepts to Gas
and Hazardous Liquid Transmission
Pipelines — Task 3**

**TEXAS TRANSPORTATION INSTITUTE
THE TEXAS A&M UNIVERSITY SYSTEM
COLLEGE STATION, TEXAS**

in cooperation with the
U.S. Department of Transportation
Research and Special Programs Administration
Office of Pipeline Safety

**DEVELOPMENT OF A PROCEDURE TO APPLY LEAK-BEFORE-RUPTURE
CONCEPTS TO GAS AND HAZARDOUS LIQUID TRANSMISSION PIPELINES**

by

Carl H. Popelar
Institute Engineer
Southwest Research Institute

Timothy S. Grant
Research Engineer
Southwest Research Institute

Walter L. Bradley
Professor
Texas A&M University

and

Gail Stucker
Research Associate
Texas A&M University

Research Study Title: Development of a Procedure to Apply Leak-Before-Rupture
Concepts to Gas and Hazardous Liquid Transmission Pipelines

Sponsored by the
Office of Pipeline Safety
In Cooperation with
U.S. Department of Transportation
Federal Highway Administration

December, 1997

TEXAS TRANSPORTATION INSTITUTE
The Texas A&M University System
College Station, Texas 77843-3135

1 Report No Task 3	2. Government Accession No.	3 Recipient's Catalog No	
4 Title and Subtitle DEVELOPMENT OF A PROCEDURE TO APPLY LEAK-BEFORE- RUPTURE CONCEPTS TO GAS AND HAZARDOUS LIQUID TRANSMISSION PIPELINES (TASK 3)		5 Report Date December 28, 1996	
		6 Performing Organization Code	
7 Author(s) Carl Popelar, Timothy Grant, Walter Bradley, and Gail Stucker		8 Performing Organization Report No Task 3	
9 Performing Organization Name and Address Texas Transportation Institute The Texas A&M University System College Station, Texas 77843-3135		10 Work Unit No (TRAIS)	
		11 Contract or Grant No Contract no DTRS56-95-C-0003	
12. Sponsoring Agency Name and Address COTR: U.S. Department of Transportation Research and Special Programs Administration Office of Pipeline Safety (DPS-13) 400 Seventh Street, SW, Room 2335 Washington D C. 20590-0001 ATTN: Mr. Gopala Vinjamuri		13 Type of Report and Period Covered Final June 1995 to September 1996	
		14 Sponsoring Agency Code	
15 Supplementary Notes			
<p>damage</p>			
17. Key Words Pipelines , Leak-Before-Rupture, Hazardous Materials, Pipeline Cracks		18. Distribution Statement No restrictions.	
19. Security Classif.(of this report) Unclassified	20. Security Classif.(of this page) Unclassified	21. No. of Pages 79 ..	22. Price

DISCLAIMER

The contents of this report reflect the findings and views of the authors who are responsible for the facts and the accuracy of the data presented herein. The contents do not necessarily reflect the official view or policies of The Office of Pipeline Safety or The Texas Department of Transportation. This report does not constitute a standard, specification, or regulation.

ACKNOWLEDGMENT

This research was sponsored by the Office of Pipeline Safety, Research and Special programs Administration, U.S. department of Transportation. The research was performed in co-operation with Dr. Carl S. Popelar, South West Research Institute, San Antonio, Texas, and with the assistance of Dr. Melvin F. Kanninen, MFK Consulting Services, San Antonio, Texas. Mr. Gopala (Krishna) Vinjamuri, Office of Pipeline Safety, Contracting Officer's Technical representative provided guidance in the preparation of the final report.

TABLE OF CONTENTS

	Page
LIST OF FIGURES	v
LIST OF TABLES	viii
SUMMARY	ix
1 INTRODUCTION	1
1.1 Background	1
2 GAS PIPELINES	4
2.1 Technical Background	4
2.2 Development of a Leak-Before-Rupture Criterion	5
2.2.1 Determination of Fracture Propagation Driving Forces	5
2.2.2 Determination of Fracture Propagation Resistance Values	6
2.2.3 Establishment of a Leak-Before-Rupture Criterion	21
2.3 Conclusions and Recommendations for Gas Pipelines	26
3 HAZARDOUS LIQUID PIPELINES	30
3.1 Technical Background	30
3.2 Analysis for Leak-Without-Rupture for Hazardous Liquid Pipelines: Case I-Avoiding Immediate Rupture at First Formation of a Through- Wall Crack	32
3.3 Analysis of Leak-Without Rupture for Hazardous Liquid Pipelines: Case II -- Time Dependent Stable Growth of a Through-Wall Crack Leading to Unstable Crack Growth and Rupture	42
3.3.1 Calculation of J-integral Driving Force for Crack Growth as a Function of Crack Length	44
3.3.2 Determination of Critical Crack Length from Calculated J-a Curves and Measured J-R Curves	47
3.3.3 Calculation of the Crack Opening Area for Axial Through-Cracks	47
3.3.4 Calculation of the Leakage Rate for Axial Through-Cracks	53
3.3.5 Relationship Between Leakage Detection Limits and Limiting Pipe Pressures to Avoid Rupture	53
3.4 Conclusions and Recommendations for Hazardous Liquid Pipelines	56
References	61

LIST OF FIGURES

		Page
Figure 1	Variation of $CTOA$ with crack speed for different initial hoop stresses in a 30-inch diameter, X52 steel pipe with a 0.375-inch wall thickness.	7
Figure 2	Variation of $CTOA$ with crack speed for different initial hoop stresses in a 30-inch diameter, X60 steel pipe with a 0.375-inch wall thickness.	8
Figure 3	Variation of $CTOA$ with crack speed for different initial hoop stresses in a 24-inch diameter, X52 steel pipe with a 0.312-inch wall thickness.	9
Figure 4	Variation of $CTOA$ with crack speed for different initial hoop stresses in a 24-inch diameter, X60 steel pipe with a 0.312-inch wall thickness.	10
Figure 5	Variation of $CTOA$ with crack speed for different initial hoop stresses in a 24-inch diameter, X52 steel pipe with a 0.375-inch wall thickness.	11
Figure 6	Variation of $CTOA$ with crack speed for different initial hoop stresses in a 24-inch diameter, X60 steel pipe with a 0.375-inch wall thickness.	12
Figure 7	Variation of $CTOA$ with crack speed for different initial hoop stresses in a 16-inch diameter, X52 steel pipe with a 0.312-inch wall thickness.	13
Figure 8	Variation of $CTOA$ with crack speed for different initial hoop stresses in a 16-inch diameter, X60 steel pipe with a 0.312-inch wall thickness.	14
Figure 9	Variation of $CTOA$ with hoop stress for X52 and X60 steels and $D/t = 80$ and 77.	16
Figure 10	Variation of the coefficient B in Equation (4) with D/t .	17
Figure 11	Comparison of fit for $(CTOA)$, of Equation (5) with computed values for X52 and X60 steels.	18
Figure 12	Comparison of fit for $(CTOA)$, of Equation (5) with computed values for X52, X60, X70 and X80 steels.	19
Figure 13	Cumulative distribution function for $(CTOA)$, and Weibull fit for X52 steel.	24
Figure 14	Cumulative distribution function for $(CTOA)$, and Weibull fit for X60 steel.	25

Figure 15	Probability of rupture as a function of the hoop stress for X52 steel pipes having different diameter to thickness ratios D/t .	27
Figure 16	Probability of rupture as a function of the hoop stress for X60 steel pipes having different diameter to thickness ratios, D/t .	28
Figure 17	Critical flaw sizes in 30-inch diameter x 0.375-inch thick (762 x 9.5mm) X52 (Grade 358) pipe compared to experimental data.	31
Figure 18	Results of leak-without-rupture analysis for various ratios of dynamic and quasi-static critical stress intensities and for ratios of initial pressure before leak P_o and after leak but before rupture P_r . If a given crack with an initial c/t and a/t value lies below the appropriate curve for a given “f” value, the leak-without-rupture occurs. Above the same curve corresponds to leak-with-rupture.	34
Figure 19	Results of leak-without-rupture analysis for various ratios of dynamic and quasi-static critical stress intensities and for ratios of initial pressure before leak P_o and after leak but before rupture P_r . If a given crack with an initial c/t and a/t value lies below the appropriate curve for a given “f” value, the leak-without-rupture occurs. Above the same curve corresponds to leak-with-rupture..	35
Figure 20	Results of leak-without-rupture analysis for various ratios of dynamic and quasi-static critical stress intensities and for ratios of initial pressure before leak P_o and after leak but before rupture P_r . If a given crack with an initial c/t and a/t value lies below the appropriate curve for a given “f” value, the leak-without-rupture occurs. Above the same curve corresponds to leak-with-rupture..	36
Figure 21	Results of leak-without-rupture analysis for various ratios of dynamic and quasi-static critical stress intensities and for ratios of initial pressure before leak P_o and after leak but before rupture P_r . If a given crack with an initial c/t and a/t value lies below the appropriate curve for a given “f” value, the leak-without-rupture occurs. Above the same curve corresponds to leak-with-rupture.	37
Figure 22	Stress intensity as a function of a/t for a pipe with a part-through crack, with $2c= 4$ “or 6””, for an internal pressure that is equivalent to 72% SMYS.	39
Figure 23	Schematic indicating the transition temperature as a function of loading rate (dynamic or static) and as a function of notch aquity (standard V-notch or fatigue precracked).	41
Figure 24	Stress required to give either pop-through of a part-through crack	43

(curves labeled K_{Ic}) or continued growth (curves labeled K_d). For a given stress and a/t value and initial flaw length $2c$, if the stress required to give “crack pop-through) is larger than the stress required to cause the crack to continue to grow, then leak-with-rupture occurs. Note all curves are elevated **as** the value of critical stress intensity is increased, as can be seen by comparing the two curves for $K_d=40$ and $120 \text{ Ksi (in)}^{0.5}$.

Figure 25	Ramberg-Osgood fit to tensile test data for X52 and X60 steel.	46
Figure 26	Calculated J-c for X52 and X60 steel with a diameter of 30” and a wall thickness of 0.375 in.	48
Figure 27	J-resistance (J-R) curves from measurements on X52 and X60 steel. The deformation J, was used in this work.	49
Figure 28	Determination of the critical crack length at which unstable crack growth and rupture occurs, using J-c calculated and J-delta-c as measured.	50
Figure 29a	Leakage rate (% of flow) versus hoop stress/yield strength for various D/t ratios for X52 steel.	57
Figure 29b	Leakage rate (% of flow) versus hoop stress/yield strength for various D/t ratios for X60 steel.	58

LIST OF TABLES

		Page
Table 1	Values and basis of the design factor in the U.S. Pipeline Safety Regulations.	2
Table 2	Computed values of $(CTOA)_{,,}$ in degrees for selected X52 steel pipes.	15
Table 3	Computed values of $(CTOA)_{,,}$ in degrees for selected X60 steel pipes.	15
Table 4	Computed $(CTOA)$, from measured 2/3-size charpy v-notch energy for X52 steels using equation (10).	22
Table 5	Computed $(CTOA)$, from measured 2/3-size charpy v-notch energy for X60 steels using equation (10).	23
Table 6	Critical crack lengths, $2c_o$, at which an axial through-crack will give unstable crack growth and rupture for various pipe geometries and steels (X52 and X60).	51
Table 7	The crack opening area for various pipe geometries with axial through-cracks that have reached critical crack length for various internal pressures.	54
Table 8	Leakage rates for various pipes at critical cracks $2c_o$ for four different internal pressures.	55
Table 9	Leakage rates (% of flow) as a function of σ_t/σ_y ratio for pipes with through-cracks of critical lengths.	59

SUMMARY

This research investigated the U.S. Code of Federal Regulations (CFR) for the maximum allowable operating pressure of transmission pipelines. In particular, the appropriate regulations are detailed in 49CFR Part 192-Transportation of Natural and Other Gases by Pipeline - Minimum Federal Standards and 49CFR Part 195 - Transportation of Hazardous Liquid by Pipeline. The current CFR regulations may not preclude large-scale rupture of gas pipelines or large-scale leakage from a hazardous liquid pipeline due to unstable growth of a through-crack. The specific objective of this research was to develop procedures to apply fracture mechanics concepts, in particular leak-before-rupture, to hazardous liquid and gas pipelines. Researchers studied under what circumstances catastrophic failures can occur in pipelines which have been designed and are operated according to pipeline safety regulations, but have developed part-through cracks due to third party damage and/or fatigue, corrosion, or stress corrosion cracking.

Southwest Research Institute addressed the gas transmission pipeline problem in two parts. First, a set of parametric computations which include the behavior of the gas during decompression was performed to quantify the driving force for steady-state crack growth of a through-wall crack in a pipe using the crack tip opening angle (*CTOA*) as the characterizing parameter for the driving force. The *CTOA* was calculated for various combinations of pipe diameter, wall thickness, and initial hoop stress for both X52 and X60 steel. Second, the fracture propagation resistance properties of older X52 steels and more modern X60 steels were determined using available Charpy V-notched impact tests to determine the critical crack tip opening angles (*CTOA*) of these materials. These results were used together to determine the minimum hoop stress and associated operating pressure necessary to sustain a long-running crack (i.e., a large-scale rupture). Because of the large variation in the fracture resistance properties for line pipe steels, a probabilistic analysis was performed to establish the probability of rupture. For pipelines transporting natural gas, it was found that if a breach of the pipe wall of sufficient size were to occur, fracture propagation is unlikely for pipe operation at the maximum allowable operating pressure in Class 4 locations, marginally likely in Class 3 and Class 2 locations but very likely in Class 1 locations. The probability of rupture decreases with decreasing pipe diameter to wall thickness ratio and with an increasing fracture toughness for the pipeline material. Conclusions are based on Charpy data sets for X52 and X60 steels which may not be representative of all X52 and X60 steels in service. The conclusions drawn then would apply only to steels with similar Charpy values.

The hazardous liquid pipeline problem has been addressed at Texas A&M University. Two approaches have been taken in the analysis of the hazardous liquid pipeline. Typical through cracks which result in leakage in hazardous liquid pipelines are on the order of 6" or less in length at the time the part-through crack becomes a through crack. Rupture, which we define as being the subsequent growth of this crack to a length of 18" or more, can occur in one of two ways: (1) the part-through crack penetrates the wall of the pipe and continues its unstable growth axially to a length of 18" or (2) the part-through crack penetrates the wall of the pipe and arrests but subsequently grows stably by fatigue or stress corrosion cracking to a length that again allows unstable crack growth to a length longer than 18". The difference between "leak" and "rupture" in our definition is obviously a matter of degrees. A short through crack (~6" or less in length) is assumed to give a modest amount of leakage but sufficient to allow detection. A crack length of

greater than 18" in the assumed definition of the rupture case gives a larger amount of leakage with more serious consequences.

The first approach mentioned above is a classical leak-before-break analysis, for which we followed the standard treatment in *Advanced Fracture Mechanics* (Kanninen and Popelar, 1985). This analysis indicates that axial growth of the crack after it penetrates the wall of the pipe depends on the square of the ratio of the pipe pressure before and after the wall is penetrated (which may be assumed to be 1.0 in a worst case scenario) and the square of the ratio of the dynamic stress intensity of the through crack, K_d , to the quasi-static fracture toughness of the pipe under plane-strain conditions, K_{Ic} . The lack of availability of appropriate fracture mechanics data at usual minimum service temperatures for older pipeline steels such as X52 hampered the analysis. Nevertheless, some representative values of fracture toughness have been assumed to illustrate the approach and indicate what operating pressures (or hoop stresses) might be suggested by such an analysis.

The second approach mentioned above uses a J-integral analysis to calculate a critical axial-through-crack length for quasi-static initiation of unstable crack growth, where a part-through-crack pops through the wall, forming a stable through-crack which subsequently grows to the critical length by fatigue or stress corrosion cracking. A parametric study was conducted to determine the driving force for crack propagation for a through-wall crack in a liquid pipeline as a function of pipe diameter, wall thickness, operating pressure and length of the through-wall crack. The J-integral has been used as the characterizing parameter for the driving force. Crack growth resistance curves from the literature (J-R curves) for X52 and X60 steel have been used in combination with the calculated J driving force for crack growth to determine the crack length at which unstable cracking occurs as a function of the hoop stress (or operating pressure). The leakage rate which would precede unstable crack growth in the liquid pipeline for a pipe with a crack at the critical size has been calculated. A higher rate of leakage corresponding to a larger critical crack size enhances the possibility of detection of the crack before unstable crack growth results in a much larger crack and a much greater leakage of product.

For hazardous liquid pipelines, X60 steel, which has a very good toughness as measured by resistance to crack growth in a J-R curve, would appear to give leakage rates as a percentage of throughput that would be easily found prior to rupture for various hoop stresses. On the other hand, the X52 steel, which has a much lower resistance to crack growth than X60, gives leakage rates at the critical flaw-size that are at or below 8% of throughput. Eight percent is estimated to be the level of reliable detection, based on discussions with engineers from the pipeline industry, for three of the four diameter to thickness ratios considered for a hoop stress of 0.72 SMYS. These pipelines would appear to be at risk to develop through-cracks that could grow undetected to a size sufficient to give rupture. However, if the period of time between the formation of a through-crack and its growth to a critical size to give rupture is sufficiently long, as it might well be, then the cumulative leakage may still give ample opportunity for the existence of a through-crack to be detected prior to catastrophic rupture.

1. INTRODUCTION

The approximately 400,000 miles of natural gas and liquid transmission pipelines in the United States are subject to third party mechanical impact damage, as well as to corrosion and fatigue. The breach of a pipe wall from any combination of these causes – as has occurred in a number of petroleum product pipelines investigated by the National Transportation Safety Board (NTSB) [1] – is a serious public safety concern. Potential exists in natural gas pipelines for a long-running dynamic fracture propagation event (i.e., a rupture) of the kind that, for example, occurred at Edison, New Jersey, in 1993 [2]. While decompression in a pipeline prevents long running cracks, a typical part-through crack that goes unstable will form a 5-6" through crack that can subsequently propagate to a length of 18" or longer, releasing a large amount of product to the environment. Consequently, in both natural gas and hazardous liquid pipelines, a rupture (i.e., long-running crack in natural gas pipeline or axial crack - 18" or greater in length in hazardous liquid pipeline) represents a significantly more serious situation than does a leak.

While certainly not frequent, accidents featuring large-scale fracture propagation events produce consequences beyond the egress of the fluid being transported. Fires and fragmentation can endanger property and lives in the vicinity of the right of way, replacing multiple sections of line pipe can be costly, and revenue can be lost due to the interruption of service during the down time needed to restore the line. Concern has therefore surfaced in the wake of the Edison, NJ, incident about whether current Department of Transportation pipeline safety regulations protect against this type of event. This research addresses the factors pertinent to pipelines failures that result in leaks and ruptures, and toughness criteria that can define leak-before-rupture in gas and hazardous liquid pipelines. It also attempts to define operating conditions which would give leak without immediate rupture and would enable the detection of product discharge by leakage well before catastrophic rupture occurs.

1.1. BACKGROUND

The purpose of this research effort has been to determine if it is likely that pipelines operated under the Code of Federal Regulations 49 CFR, Parts 192 and 195 regulation for pipelines, might rupture [3]. The leak-before-rupture concept used in this study accepts the possibility that part-through cracks can develop in service due to third party damage, corrosion, stress corrosion cracking, and/or fatigue. In time, a part-through crack may grow to a critical size and breakthrough the pipe wall to cause either a leak or a rupture (unstable crack propagation). Developing procedures that will help avoid the unstable growth of such cracks which will produce rupture (rather than just leakage) is the goal of this research.

For gas transmission pipelines, the U.S. Code of Federal Regulations (CFR), ~~Part~~ 192 prescribes maximum allowable operating pressure (**MAOP**). Omitting the joint factor and the temperature derating factor, which are equal to unity in most conditions, the governing relation gives [3]

$$p = F(2St/D) \quad (1)$$

where p is the maximum allowable operating pressure, S is the yield strength, D is the nominal diameter of the pipe, t is the nominal wall thickness, and F is the design factor. The design factor, which is set forth in Section 192.111, depends upon the particular surroundings of the pipe right of way and will therefore depend upon the pipeline location as shown in Table 1. The design factors used for hazardous liquid pipelines are in Section 195.106 with an F value of 0.72 for pipelines on land, 0.6 for pipe used offshore, and 0.54 for pipe that has been subjected to cold expansion to meet the minimum yield requirements [3]. There are no class locations for hazardous liquid pipelines.

Table 1. Values and basis of the design factor in the U.S. Pipeline Safety Regulations: 49 CFR, Section 192.5 for Transportation of Natural and Other Gas by Pipeline

1	0.72	Any class location unit that has 10 or less buildings intended for human occupation.
2	0.6	Any class location unit that has more than 10 but less than 46 buildings intended for human occupancy.
3	0.5	Any class location unit with 46 or more buildings intended for human occupancy or an area where the pipeline lies within 100 yards of either a building or playground occupied by 20 or more persons....
4	0.4	Any class location unit where buildings with four or more stories above ground are prevalent.

Mechanical damage inflicted by third parties, general corrosion, and fatigue loadings due to pressure fluctuations can result in relatively short through cracks and leakage. Usually axially oriented cracks **are** potentially the most onerous. If the resulting through-wall crack is relatively short, a leak-without-rupture is likely to occur. On the other hand, if the resulting through-wall crack is sufficiently long, the crack can propagate a considerable distance leading to rupture of the pipe. Pressurized natural gas pipelines are particularly vulnerable to this type of failure because the compressed gas can expand, maintaining the pressure in the pipeline despite leakage, giving a sustained crack driving force. Incompressible liquids, on the other hand, will decompress before unstable crack growth can occur over a longer distance, and thus, will not produce the long dramatic failures associated with natural gas pipeline ruptures. Whether a throughwall-crack will experience subsequent unstable crack growth depends upon the compressibility of the fluid in the pipe, the operating pressure, the size of the pipeline, and the fracture toughness of the pipe material.

If through-wall cracking occurs, a leak with tolerable consequences is preferable to a rupture and attendant uncontrolled flow. Office of Pipeline Safety regulations were not developed to address the effects of through-wall cracks, much less discern whether a leak or rupture is likely.

Historically, a number of empirical relations have been developed for use in designing and operating gas transmission pipelines without risk of a rupture [4]. Being empirical relations, they suffer from the lack of a proper theoretical foundation. When used to interpolate within the database from which they were constructed, they yield reasonable predictions, even though the dependence of each relation on the parameters can vary significantly. They can lead to nonconservative predictions (i.e., predicting leak when rupture occurs) when used to extrapolate to conditions outside the database from which they were developed. The empiricism of these relations makes it virtually impossible to establish definitive guidelines and/or limitations.

Because depressurization process is distinctly different in liquid and gas pipelines, leak-without-rupture issues and methodology are different. Thus, report is divided into two sections to address natural gas pipelines and hazardous liquid pipelines separately.

2. GAS PIPELINES

2.1 Technical Background

The basic principles of dynamic fracture propagation have been extensively studied by various researchers [5-6]. However, applying these principles is generally not routine. It is particularly complex for gas transmission pipelines for two reasons. First, in a gas pipeline the dynamic crack driving force arises from the intimately inter-connected deformation of the pipe wall, the fluid motion as it decompresses and escapes from the pipe, and the speed of the crack. Second, because modern pipelines are generally made of ductile and tough steels, the resistance to dynamic crack propagation will be significantly affected by the plastic deformation of the material at the crack tip as the crack advances.

The problem as applied to pipelines has been simplified in previous work [7] by reasoning that a long-running crack propagation process must be one that occurs in a steady-state mode that is independent of its origin. This makes it possible to decouple the steady-state dynamic fracture propagation process from its quasi-static precursors – the initial wall break-through and the subsequent transient stage of the axial crack propagation. Accordingly, by concentrating on steady-state dynamic axial crack propagation, the conditions that preempt or terminate this process can be quantified with an existing fluid/structure/fracture-interaction computer model. The key assumption is that preventing steady-state crack propagation precludes long-running fractures.

To develop these guidelines researchers used SwRI proprietary computer code known as PFRAC, an acronym for Pressure-boundary Fracture Research Analysis Code. Reference [7] and a sequence of reports cited therein describe this code and its validation by critical comparisons with full-scale pipe fracture experiments conducted by Centro Sviluppo Materiali (CSM). With this unique computational capability, a set of parametric computations was developed that delineated the contribution of the pipe dimensions, line pipe steel properties, and gas pressures to the crack driving force. The crack tip opening angle (*CTOA*) was identified in fracture experiments performed by CSM and SNAM [7] as being an appropriate measure of the inelastic crack driving force in dynamic ductile fracture of line pipe and is computed with PFRAC. A key finding was that, over the range of possible steady-state crack speeds, there is always a maximum value of the *CTOA*, denoted as $(CTOA)_{max}$, for specified pipe size, mechanical properties, and initial line pressure.

Briefly, the Peng-Robinson cubic equation of state is employed to calculate the speed of sound in the gas mixture from its pressure and density which in turn is used in developing the decompression pressure at the crack tip as a function of the crack speed. Equations for the decay of the fluid pressure aft of the crack tip are developed and provide the loading for the fractured pipe. The structural element in PFRAC is a bi-linear, four noded, quadrilateral element with single point quadrature. A nodal release algorithm in concert with a nodal force reduction is used to simulate numerical crack propagation between adjoining elements. The *CTOA* is computed using a substructuring technique. For prescribed pipe size, material properties and initial line pressure, this analysis is repeated for different assumed crack speeds to determine $(CTOA)_{max}$.

The process is then repeated for different pressures to obtain $(CTOA)_{cr}$ as a function of initial pressure or, equivalently, hoop stress.

The second key result of the SwRI, CSM and SNAM work is a procedure for determining the material property counterpart of **the** $CTOA$; i.e., the critical crack tip opening angle, $(CTOA)_{cr}$. As described in Reference [7], $(CTOA)_{cr}$, expressed in degrees, for a bend fracture specimen is given by

$$(CTOA)_{cr} = 2.571 \frac{S_c}{\sigma_{od}} \frac{180}{\pi} \quad (2)$$

in which S_c is the gradient of specific absorbed energy E with respect to the specimen ligament length, described in more detail in Section 2.2.2. The average dynamic flow stress σ_{od} is taken to be $\sigma_{od} = 0.65(sY + sU)$ in which sY and sU are the yield and ultimate strengths of the material, respectively.

By specifically assuming that a leak has occurred, the focus can be conveniently placed on the use of PFRAC to quantify the conditions under which a large-scale rupture would subsequently occur. Mathematically, this is done through the fracture mechanics relation

$$(CTOA)_{cr} \geq (CTOA)_{leak} \quad (3)$$

The equality in Equation (3) defines the critical point at which a slow leak from a through-crack becomes a catastrophic rupture and is the recently proposed "leak-before-rupture" criterion for pressurized gas pipes [7]. This criterion – with suitable refinements being made to Equations (2) and (3) to account for the wide range of pipe sizes, line pipe steels, and operating pressures of interest in the current work – was used in this work to establish the limiting hoop stress for leak-before-rupture, or leak without large-scale rupture.

2.2 Development of a Leak-Before-Rupture Criterion

In this analysis the leak-before-rupture criterion is applied with the understanding that while a leak is never acceptable, it is still a less consequential failure mode than large-scale rupture; e.g., as would be associated with a long running fracture in a gas transmission pipeline. But, because a leak affords opportunities for early detection that can minimize the consequences of the failure, it is useful that guidelines that preclude large-scale rupture be established, both for older pipelines and for new construction. In this section consideration will be specifically given to both cases through a focus on X52 steels from which many older existing pipelines were fabricated, and on X60 steels that have been typically used in recent pipeline construction.

2.2.1 Determination of Fracture Propagation Driving Forces

The procedure used to develop crack driving forces for the two pipe steels for a range of pipe sizes was similar to that described in Reference [6] and outlined in the preceding section.

Specifically, using mechanical property data from the literature for X52 and X60 steels, parametric computations were made using PFRAC for specified values of pipe diameter, wall thickness, and initial gas pressure to determine $CTOA$ as a function of these parameters. This was done by selecting trial values of the steady-state crack speed spanning the range of physically possible speeds, then graphically determining the maximum value. This is $(CTOA)_{max}$. Example results for X52 steel for three hoop stress values in a 30-inch diameter, 0.375 inch wall thickness pipe transporting natural gas are shown in Figure 1. Similar results for X60 steel are provided in Figure 2 for comparison.

Figures 1 and 2 show that a readily discernible maximum value of the computed $CTOA$ occurs for each different hoop stress that was specified. Further computations were performed for 16-inch and 24-inch diameter pipes and are shown in Figures 3 - 8. Values of $(CTOA)_{max}$, derived from these computations, are summarized in Tables 2 and 3 for X52 and X60 steels, respectively.

The computational data for $D/t = 77$ and 80 , the largest values considered, are shown in Figure 9. The results for X52 and X60 are nearly consolidated into a single curve when the hoop stress is normalized with respect to its respective specified minimum yield strength $(SMYS)_{\sigma_{SMYS}}$. The fit to the data in Figure 9 is given by

$$(CTOA)_{max} = B(\sigma_H/\sigma_{SMYS})^{3/2} \quad (4)$$

This expression was also used to fit computed $(CTOA)_{,,}$ data for $D/t = 51$ and 64 . As depicted in Figure 10, the coefficient B varies linearly with D/t . The fit of the data over the entire range of D/t values considered becomes

$$(CTOA)_{,,} = (4.584 + 0.1025D/t)(\sigma_H/\sigma_{SMYS})^{3/2} \quad (5)$$

An assessment of the quality of this curve fit can be made by comparing the predictions of Equation (5) and the original PFRAC data, choosing various values for hoop stress and D/t from Figs. 1-8 to compare to the predictions of Equation (5), which attempts to summarize all of this graphical data in one analytical relationship. As can be seen in Figure 11, this is found to be entirely acceptable. However, as shown in Figure 12, it should be recognized that this interpolating relation, when extrapolated to X70 and X80 steel computational data obtained in previous work [7], is not as satisfactory for the larger values of σ_H/σ_{SMYS} .

2.2.2 Determination of Fracture Propagation Resistance Values

A two-specimen test protocol has been developed by CSM and SNAM [7] to measure the fracture resistance $(CTOA)_{,}$. In this test, bend fracture specimens having different initial ligament lengths are fractured under impact loading and the absorbed impact fracture energy is measured. The measured specific fracture energy (energy per unit of fracture surface area) includes not only energy to propagate the fracture but also to initiate propagation. Priest and Holmes [8] demonstrated that the specific impact fracture energy E can be expressed as

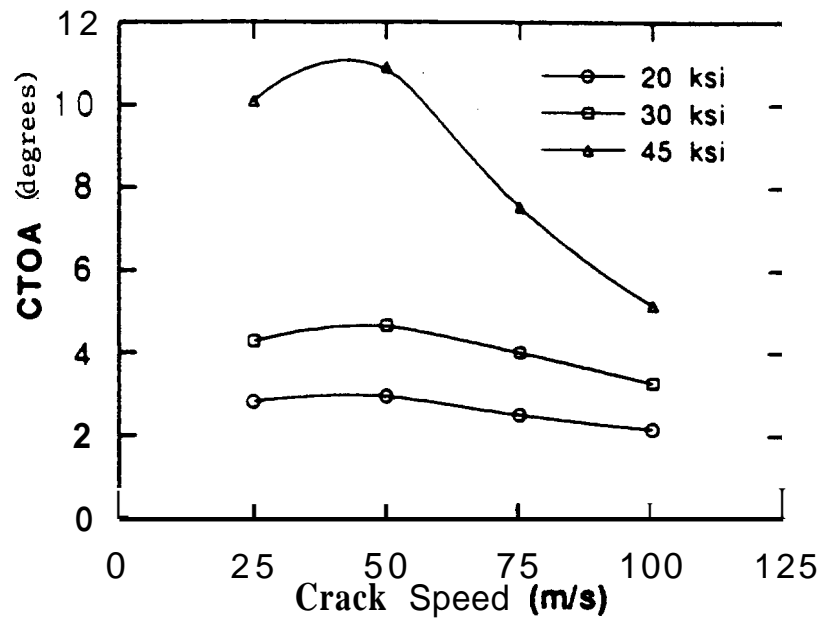


Figure 1 Variation of *CTOA* with crack speed for different initial hoop stresses in a 30-inch diameter, X52 steel pipe with a 0.375-inch wall thickness.

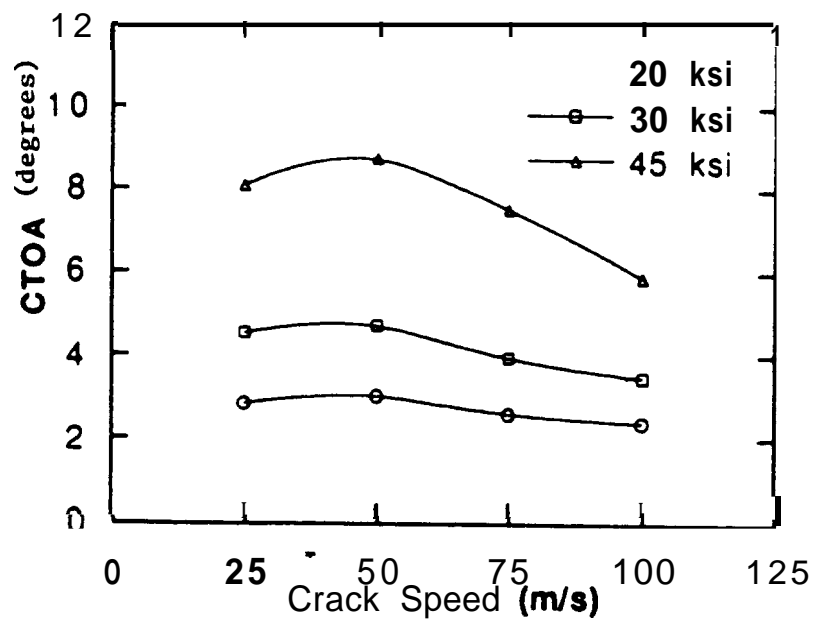


Figure 2 Variation of *CTOA* with crack speed for different initial hoop stresses in a 30-inch diameter, X60 steel pipe with a 0.375-inch wall thickness.

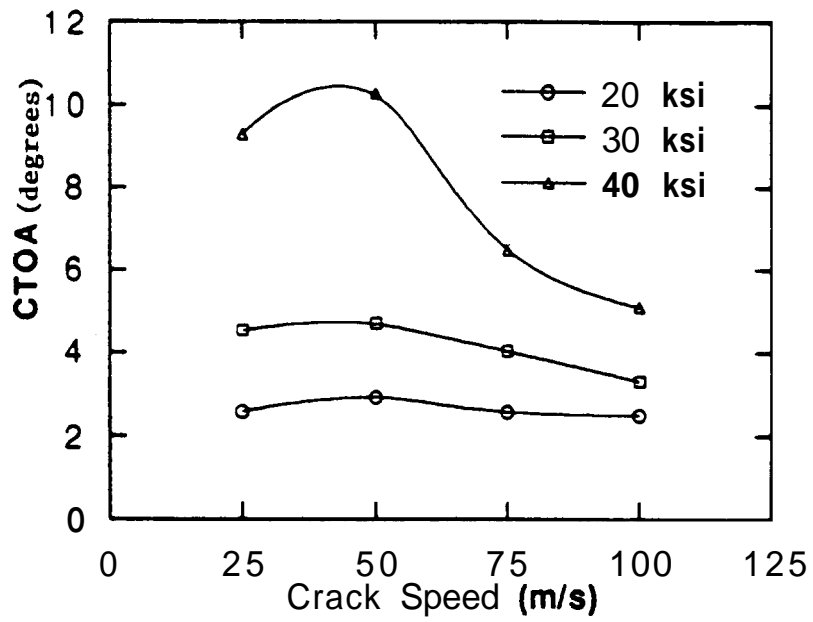


Figure 3 Variation of *CTOA* with crack speed for different initial hoop stresses in a 24-inch diameter, X52 steel pipe with a 0.312-inch wall thickness.

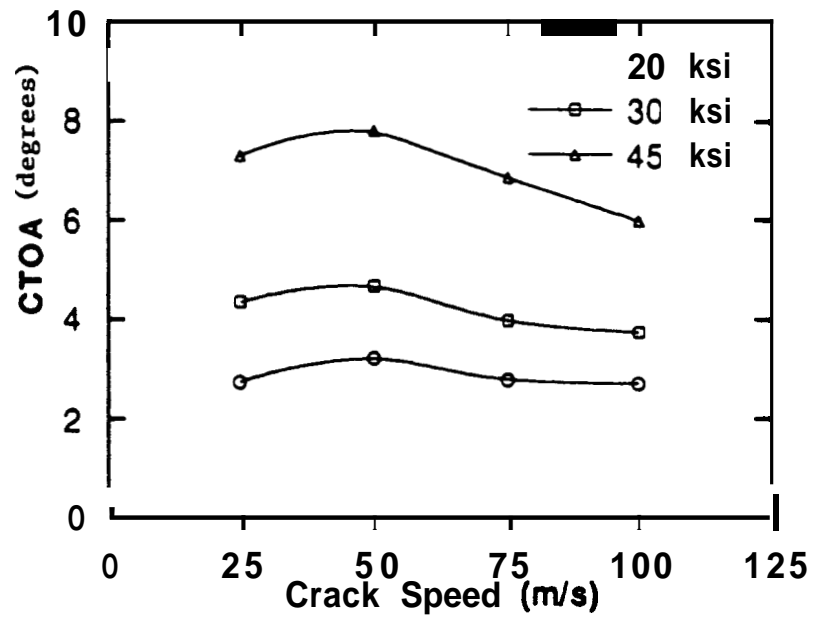


Figure 4 Variation of CTOA with crack speed for different initial hoop stresses in a 24-inch diameter, X60 steel pipe with a 0.312-inch wall thickness.

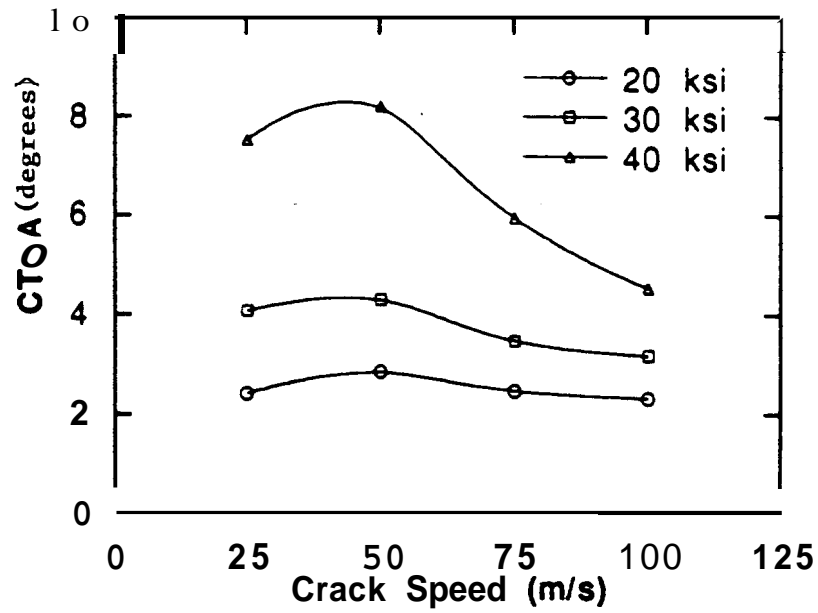


Figure 5 Variation of *CTOA* with crack speed for different initial hoop stresses in a 24-inch diameter, X52 steel pipe with a 0.375-inch wall thickness.

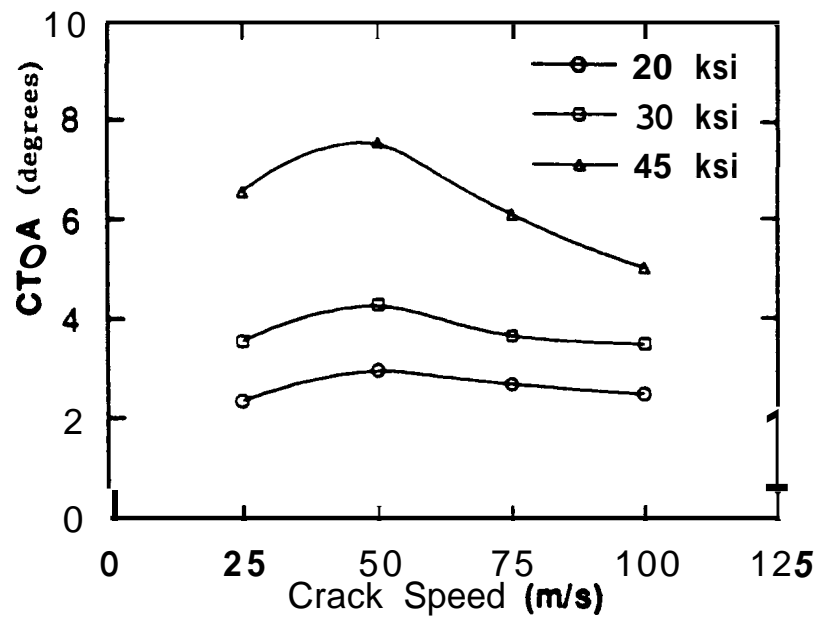


Figure 6 Variation of *CTOA* with crack speed for different initial hoop stresses in a 24-inch diameter, X60 steel pipe with a 0.375-inch wall thickness.

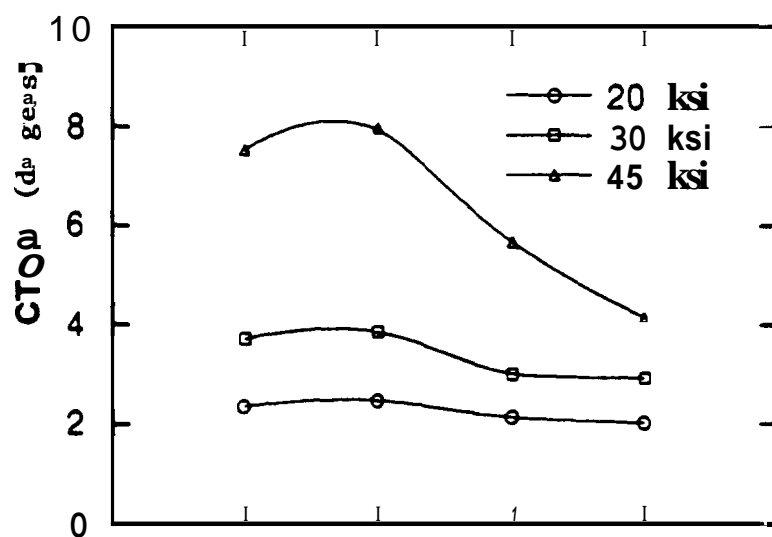


Figure 7 Variation of *CTOA* with crack speed for different initial hoop stresses in a 16-inch diameter, X52 steel pipe with a 0.312-inch wall thickness.

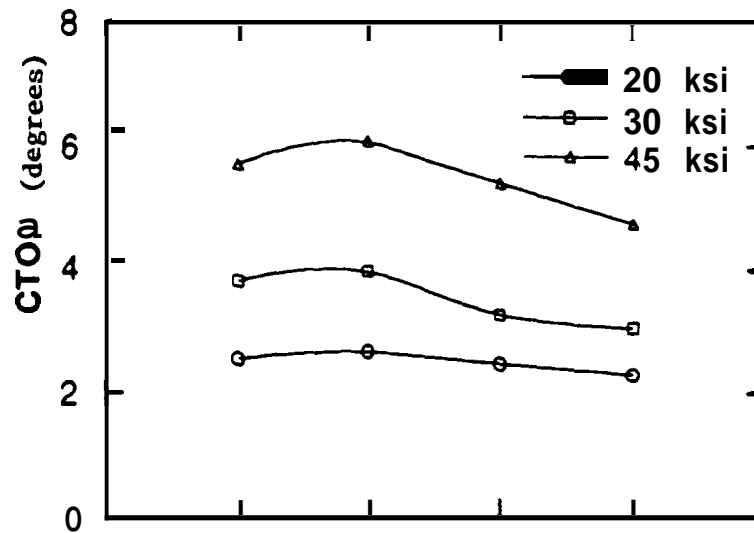


Figure 8 Variation of *CTOA* with crack speed for different initial hoop stresses in a 16-inch diameter, X60 steel pipe with a 0.312-inch wall thickness.

Hoop Stress	$D = 16$ in	$D = 24$ in		$D = 30$ in
ksi	$t = 0.312$ in	$t = 0.312$ in	$t = 0.375$ in	$t = 0.375$ in
20	2.48	2.94	2.83	2.98
30	3.85	4.71	4.28	4.68
45	7.95	10.29	8.19	10.92

Hoop Stress	$D = 16$ in	$D = 24$ in		$D = 30$ in
ksi	$t = 0.312$ in	$t = 0.312$ in	$t = 0.375$ in	$t = 0.375$ in
20	2.66	3.23	2.94	3.02
30	3.96	4.67	4.26	4.72
45	6.07	7.8	7.52	8.75

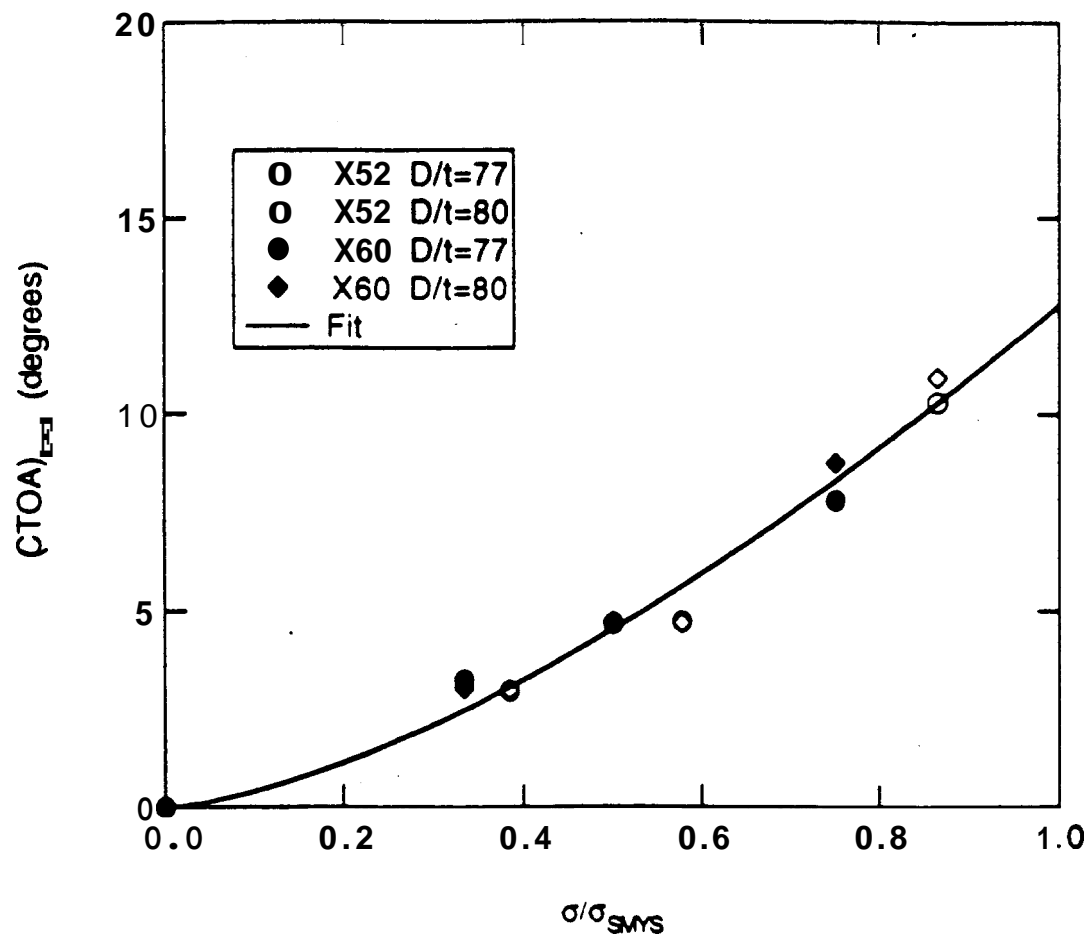


Figure 9 Variation of CTOA with hoop stress for X52 and X60 steels and $D/t = 80$ and 77.

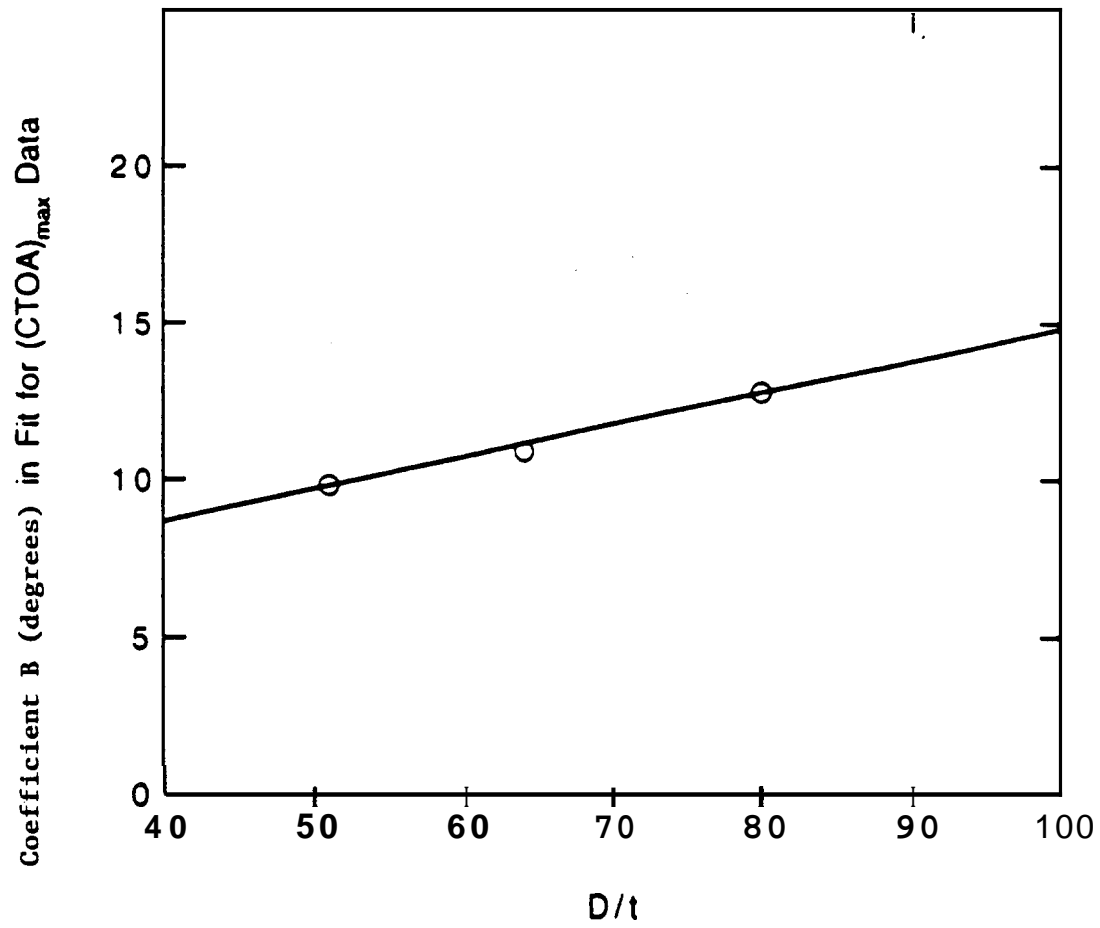


Figure 10 Variation of the coefficient B in Equation (4) with D/t .

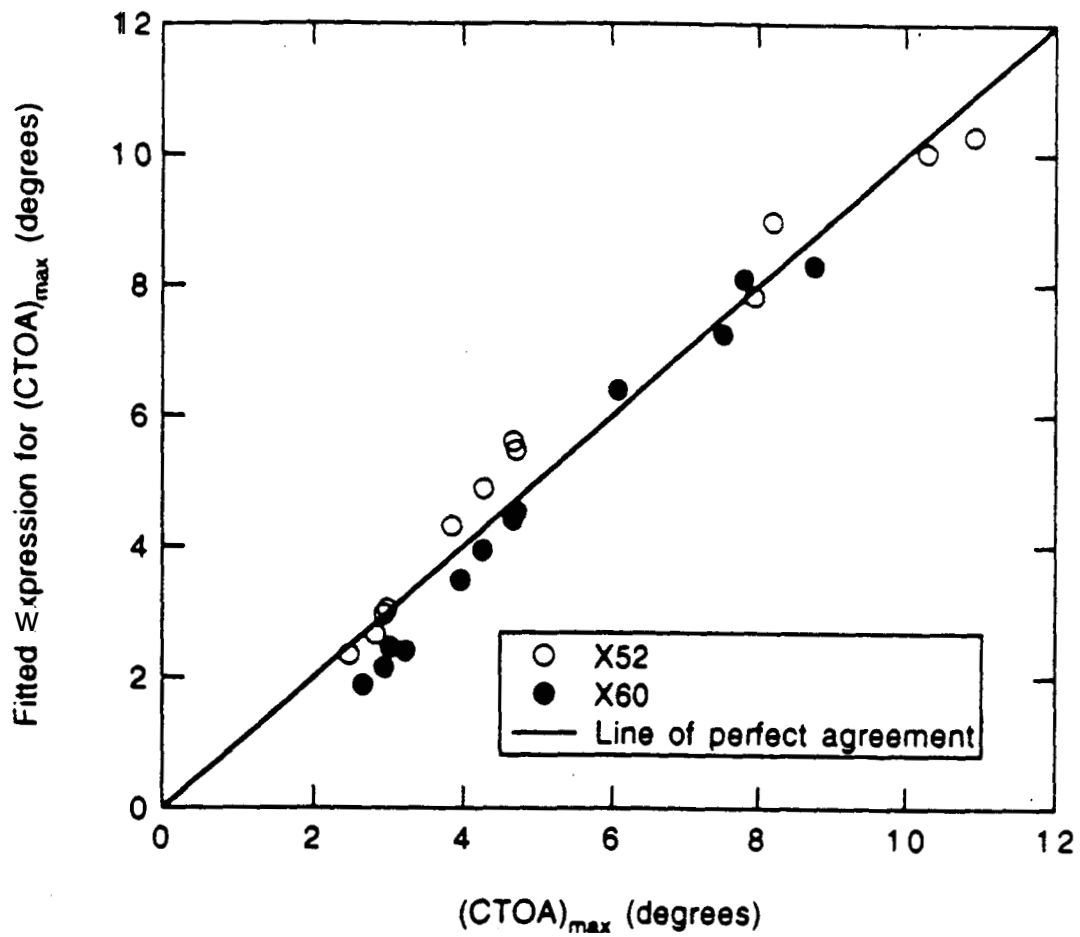


Figure 11 Comparison of fit for $(CTOA)_{max}$ of Equation (5) with computed values for X52 and X60 steels.

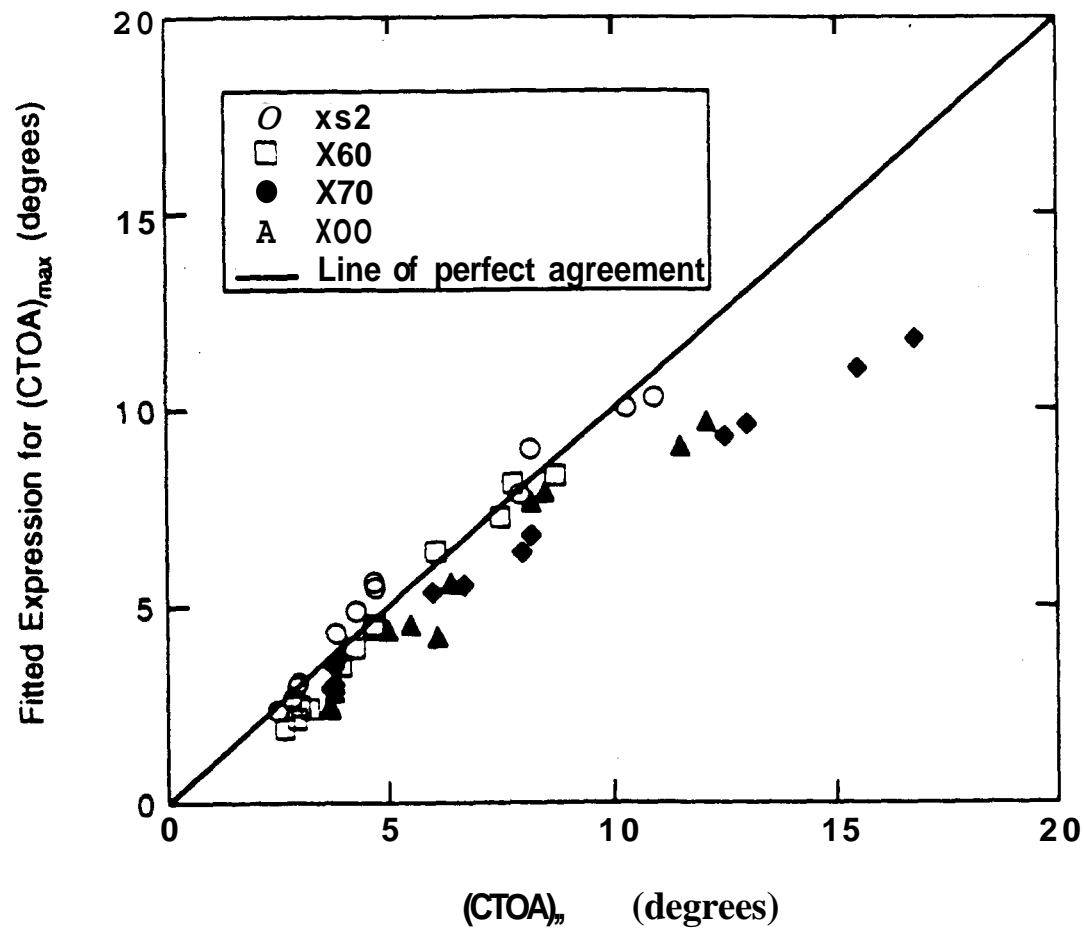


Figure 12 Comparison of fit for $(CTOA)_{max}$ of Equation (5) with computed values for X52, X60, X70 and X80 steels.

$$E = E_0 + S_c b \quad (6)$$

The specific initiation energy E_0 is observed to be virtually independent of the initial ligament length, b , of the specimen as long as “ b ” is sufficiently large to maintain full constraint.

The two-specimen test protocol for determining (*CTOA*), measures the full thickness and specific impact fracture energies for two bend specimens that are otherwise identical except that they have different initial ligament lengths or, equivalently, different lengths of initial starter cracks. If E_1 and E_2 denote the specific impact energies for two specimens having initial ligament lengths b_1 and b_2 , respectively, it then follows from Equation (6) that the gradient of specific energy is

$$S_c = \frac{E_1 - E_2}{b_1 - b_2} \quad (7)$$

Consequently, it is necessary to have samples of the material to test in order for a (*CTOA*), value to be properly determined. **As** this was not possible within the scope of the current work, an alternative approach was necessary. Moreover, the only toughness data that is available for line pipe steel in the field is the Charpy V-Notch energy; typically, for two-thirds size specimens.

The idea of using Charpy V-Notch (CVN) and Battelle drop weight tear test (DWTT) impact energies to determine S_c has been investigated in previous work [7]. Since these two test specimens are quite different in size, the use of these two specimens requires the further assumption that the specific fracture energy values in Equation (6) are independent of specimen thickness. In the one case in which this approach was tried and the results compared to those using standard test specimens to measure S_c (Eq. 7), the S_c value obtained from Charpy and DWTT was **30%** higher than that obtained from the standard test specimens [7]. However, in the absence of any alternative, CVN experimental data was used in combination with predictions of DWTT data from CVN-DWTT correlations in the literature. For X52 and X60 steel, only Charpy data for 2/3-size Charpy specimens was available. Thus, a further assumption was made that DWTT specific fracture energy could be obtained from 2/3-size Charpy data through an empirical expression [9]

$$E_{DWTT} = 3600 + 3E_{CVN} \quad (8)$$

where E_{DWTT} and E_{CVN} are, respectively, the specific impact energies in DWTT and 2/3-size CVN tests expressed in lbs/in. While this correlation was developed for line pipe steels in use prior to 1974, it provides reasonable estimates for E_{DWTT} for X65, X70 and X85 steels used in newer pipelines.

If the DWTT and CVN energies are used in Equation (7), it follows that

$$S_c = \frac{3600 + 2E_{CVN}}{b_{DWTT} - b_{CVN}} \quad (9)$$

where use has been made of Equation (8). The ligament lengths in the standard Battelle DWTT and CVN specimens are $b_{DWTT} = 2.8$ in and $b_{CVN} = 0.315$ in, respectively. The introduction of Equation (9) into Equation (2) provides the following estimate

$$(CTOA)_c = 59.28 \frac{3600 + 2E_{CVN}}{\sigma_{od}} \quad (10)$$

in which σ_{od} and E_c have the units of psi and lbs/in, respectively.

Data reported in References [10, 11] for X52 and X60 steels are summarized in Tables 4 and 5, respectively, along with $(CTOA)$, determined from Equation (10). It is clear from these tables that there are rather wide distributions for the yield and ultimate strengths, CVN energy and, hence, $(CTOA)$, for these steels. For example, the ratio of the largest reported CVN energy to its smallest is greater than two for each steel. The mean value of $(CTOA)$, is 7.2 degrees with a standard deviation of 1.1 degrees for X52 steel compared to 6.4 degrees and 1.4 degrees, respectively, for the higher strength X60 steel. It is worth noting that the average charpy value for 2/3rds size charpy specimens was -24 ft-lbs. for both X52 and X60 steel, whereas one would have expected X60 to be higher, which it is in the J-R curves to be presented later in this report.

Figure 13 depicts the cumulative distribution function (CDF), $F_x(x) = P(X \leq x)$; i.e., the probability that $X \leq x$ for X52 steel. This distribution for $(CTOA)$, is described reasonably well by a Weibull distribution

$$F_x(X) = 1 - \text{EXP}[-(X/\beta)^a] \quad (11)$$

for which the shape parameter $a = 8.25$ and the scale parameter $\beta = 7.39$. Figure 14 shows a similar comparison of X60 steel for which $a = 4.09$ and $\beta = 6.92$ provide the best least square fit of the Weibull distribution to the data. In this case, the data set is smaller and the Weibull distribution does not fit the data as well. Normal and lognormal distributions were also investigated, but they provided even less satisfactory fits.

2.2.3 Establishment of a Leak-Before-Rupture Criterion

Table 4 Computed (CTOA), from Measured 2/3 Size Charpy V-Notch Energy for X52 Steels
Using Equation 10

Test ID	Yield Strength	Ultimate Strength (psi)	2/3-CVN Energy (ft-lbs)	Specific CVN Energy (lbs/in)	CTOA _c (deg)
1*	58,700	76,100	31	4,500	8.52
2*	58,700	76,100	31	4,500	8.52
3*	58,700	76,000	31	4,500	8.52
4*	63,800	80,600	23	3,339	6.49
5	58,800	75,300	29	4,210	8.17
80*	58,600	75,500	21	3,048	6.59
81*	68,770	84,100	13	1,887	4.40
88*	61,812	79,993	24	3,484	6.89
A1/X1**	56,600	71,800	25	3,620	7.70
A2/B1**	55,800	74,200	22	3,186	7.70
A2/X5**	56,600	77,800	20	2,896	6.37
CA2/41S**	59,400	85,500	25	3,620	6.82
CA2/41M**	67,500	89,700	24	3,475	6.12
CA2/M1**	55,900	85,700	15	2,172	5.12
CA2/M4**	58,900	84,100	20	2,896	5.99
CA2/M1**	57,400	84,000	21	3,041	6.25
CA2/M3**	55,000	78,000	22	3,186	6.84
CA2**	62,500	79,900	25	3,620	6.94
A21/TF3**	52,600	67,000	27	3,910	8.71
A22**	61,600	82,300	25	3,620	6.87
A25**	56,200	79,400 *	32	4,634	8.65
A35/CQ5**	60,300	78,200	29	4,199	7.90
A35/CQ1**	61,600	81,000	26	3,765	7.12
A35/CQ5**	57,400	75,000	26	3,765	7.67
A35/CQ6**	58,500 *	76,500	23	3,331	6.93
A35/CQ3**	61,220	79,400	26	3,765	7.22

*Reference[1] **Reference[10]

Table 5 Computed (*CTOA*), from Measured 2/3-Size Charpy V-Notch Energy for X60 Steels Using Equation (10).

Test ID	Yield Strength (psi)	Ultimate Strength (psi)	2/3-CVN Energy* (ft-lbs)	Specific CVN Energy (lbs/in)	CTOA _c * (deg)
A4/M1**	71,100	93,400	21	3,041	5.37
A3/MJ**	71,900	93,400	19	2,751	5.02
A6/M2**	71,900	93,400	20	2,896	5.18
A13/T4**	65,100	79,800	33	4,779	8.28
A13/T1**	66,100	82,700	33	4,779	8.06
A21/T2**	65,800	80,600	32	4,634	8.02
A21/T3**	65,000	82,000	36	5,213	8.70
A28/AT1**	64,900	80,200	21	3,041	6.09
A28/CV4**	60,800	82,000	19	2,751	5.81
A36/CV2**	61,700	86,800	20	2,896	5.77
A36/CV1**	71,100	94,000	17	2,462	4.71
A36/CV3**	61,000	78,800	20	2,896	6.13

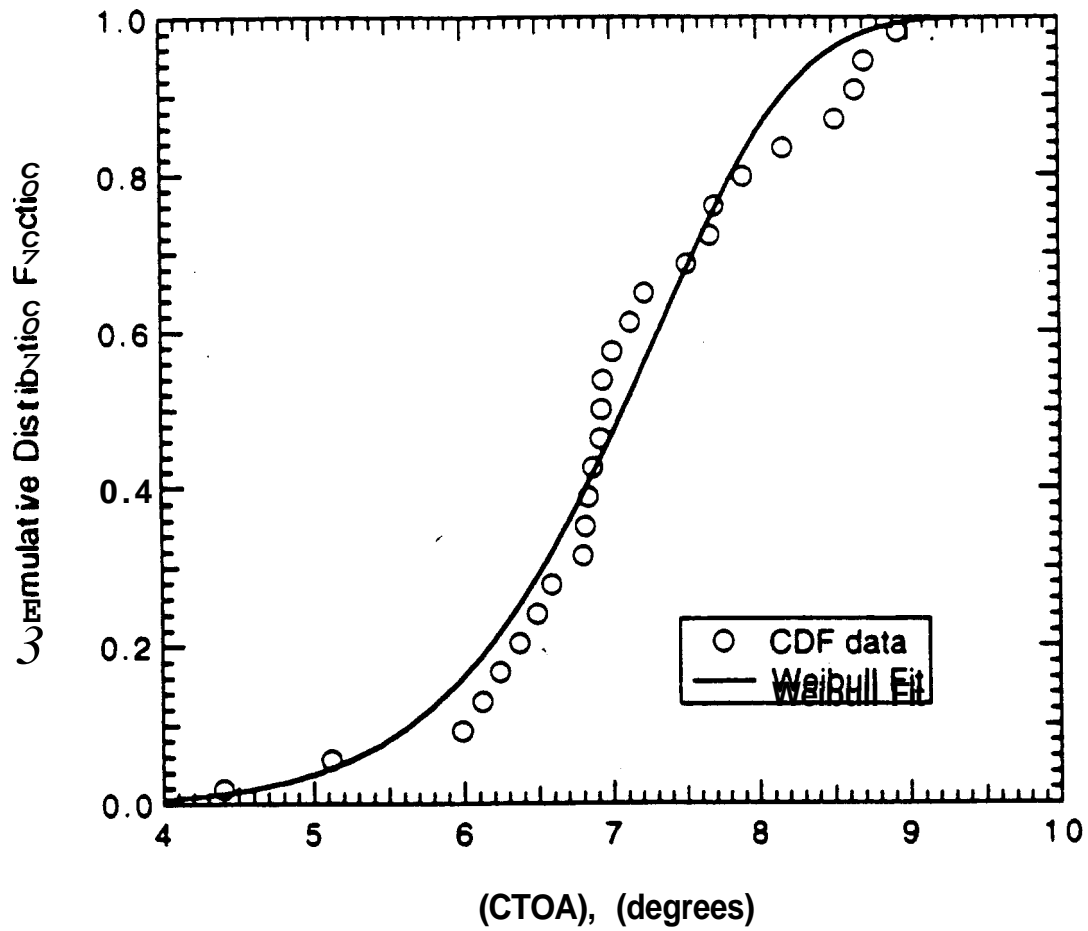


Figure 13 Cumulative distribution function for $(CTOA)_c$ and Weibull fit for X52 steel.

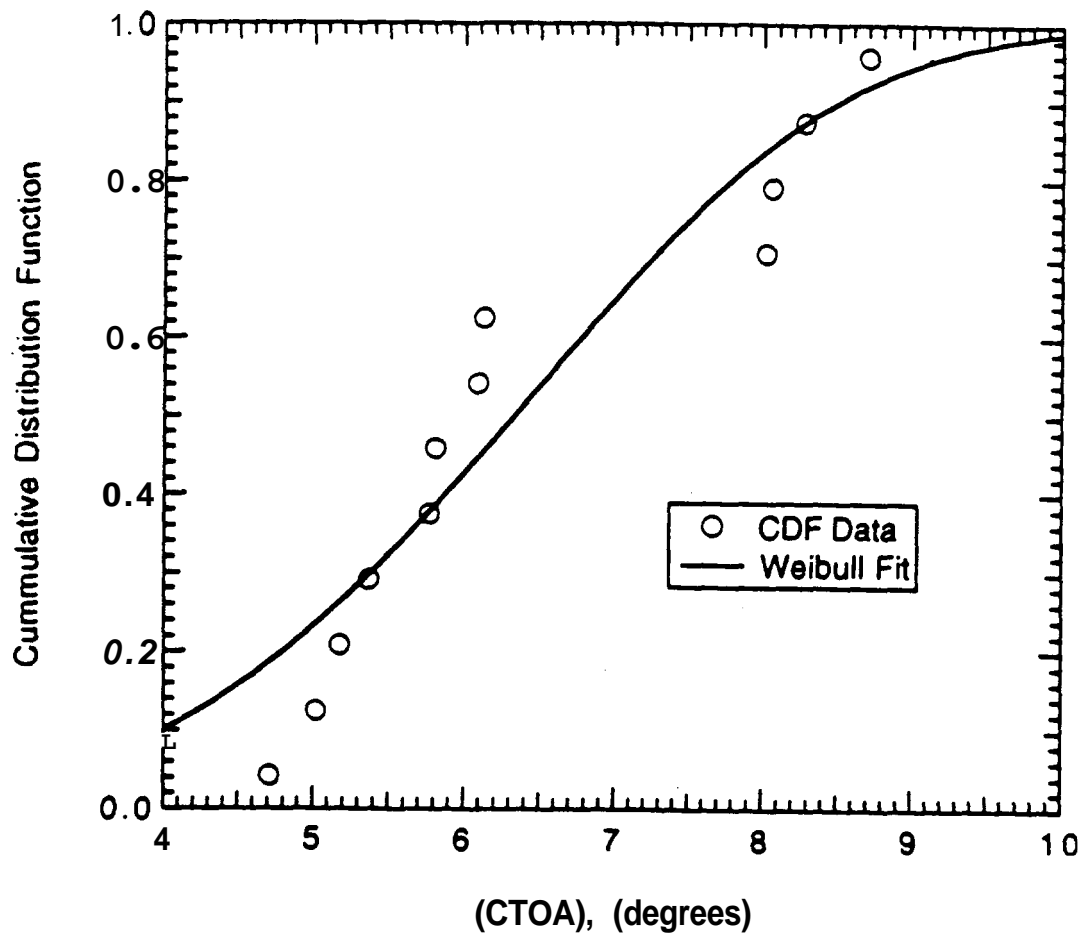


Figure 14 Cumulative distribution function for $(CTOA)_c$ and Weibull fit for X60 steel.

If $(CTOA)_c > (CTOA)_{max}$, then a long running axial crack (i.e., a rupture) is precluded and a leak will occur should a through-wall crack develop in the pipe wall. In a deterministic approach the limiting condition for a leak-before-rupture is obtained by equating $(CTOA)_c$ and $(CTOA)_{max}$. However, since rather wide variations in $(CTOA)_c$ were found, a probabilistic approach to leak-before-rupture is more appropriate. The probability of a rupture p_r , is given by

$$P_r = P[X = (CTOA)_c \leq x = (CTOA)_{max}] = F_X(x) \quad (12)$$

Note that the probability of a leak-before-rupture is $p_l = 1 - p_r$

Using Equations (5), (11), and (12) yields the probability of rupture depicted in Figures 15 and 16 for X52 and X60 steels, respectively. Also shown in these figures are vertical lines representing the design factors for the respective class locations. The point of intersection of these lines with the curves establishes the probability of rupture for the respective class location. For example, the probability of rupture for a Class 4 location ($F=0.4$) is nearly nonexistent for X52 steel or, conversely, the probability of leak-before-rupture is very high should a breach of the pipe wall occur. The probability for a leak-before-rupture is somewhat less for X60 steels. The probability that a rupture will occur for Class 1 locations is very high for X52 and X60 steels; particularly, for the larger values of D/t . Figures 15 and 16 indicate a higher probability of failure for higher D/t values. This should be thought of as a diameter effect (and not a wall thickness effect), since energy storage in the contained gas is greater for a given amount of pipe material where D/t is larger. The potentially important effect of wall thickness, t , on the $(CTOA)_c$ is not addressed. Implicitly, it has been assumed that $(CTOA)_c$ is not a function of the wall thickness of the pipe.

2.3 Conclusions and Recommendations for Gas Pipelines

The research described herein was undertaken to investigate the possibility that the current CFR regulations for the maximum allowable operating pressure (**MOP**) of a natural gas transmission pipeline do not preclude a large-scale rupture. This was accomplished by work on two aspects of the problem. First, a set of parametric computations was performed that have established the conditions under which a sufficiently long, part-through-wall crack in a pipe, occurring because of third party mechanical damage and/or corrosion and fatigue, would become a dynamically propagating fracture when it unstably penetrated the remaining portion of the pipe wall. These computations were performed for pipe diameters, wall thicknesses, and line pipe steels that are representative of the transmission pipeline network in North America. Second, the fracture propagation resistance properties of an older and a more modern line pipe steel were estimated from mechanical properties and 2/3-size Charpy V-notch impact energies.

The results of this research, provided in Figures 15 and 16, give a statistical basis for evaluating the potential leak-before-rupture for the full range of conditions in which the present system is being operated. They indicate that the risk of a dynamic fracture propagation event (i.e., a rupture) following a breach of the pipe decreases with decreasing D/t ratio and value of the design factor. Generally, in **Class 4** locations where $F = 0.4$ requiring $\sigma_h/\sigma_{SMYS} = 0.4$, there is very little risk of dynamic fracture propagation in X52 steel pipes, and only a slightly greater risk in X60 steel pipes. The risk increases as design factor F increases due to class location to the

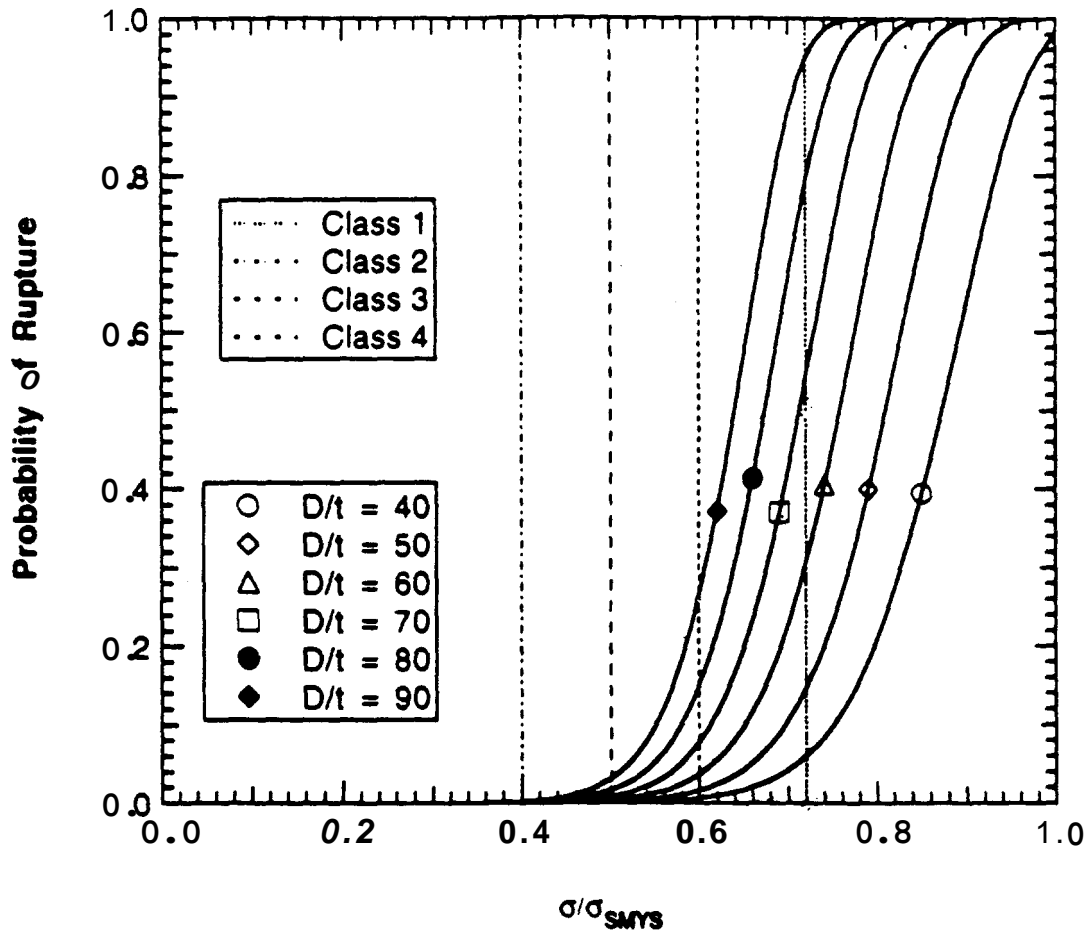


Figure 15. Probability of rupture as a function of the hoop stress for X52 steel pipes having different diameter to thickness ratios D/t . The predictions presented in this figure are specific to the Charpy data set in Table 4 and are not intended to be a prediction for all X52 steel.

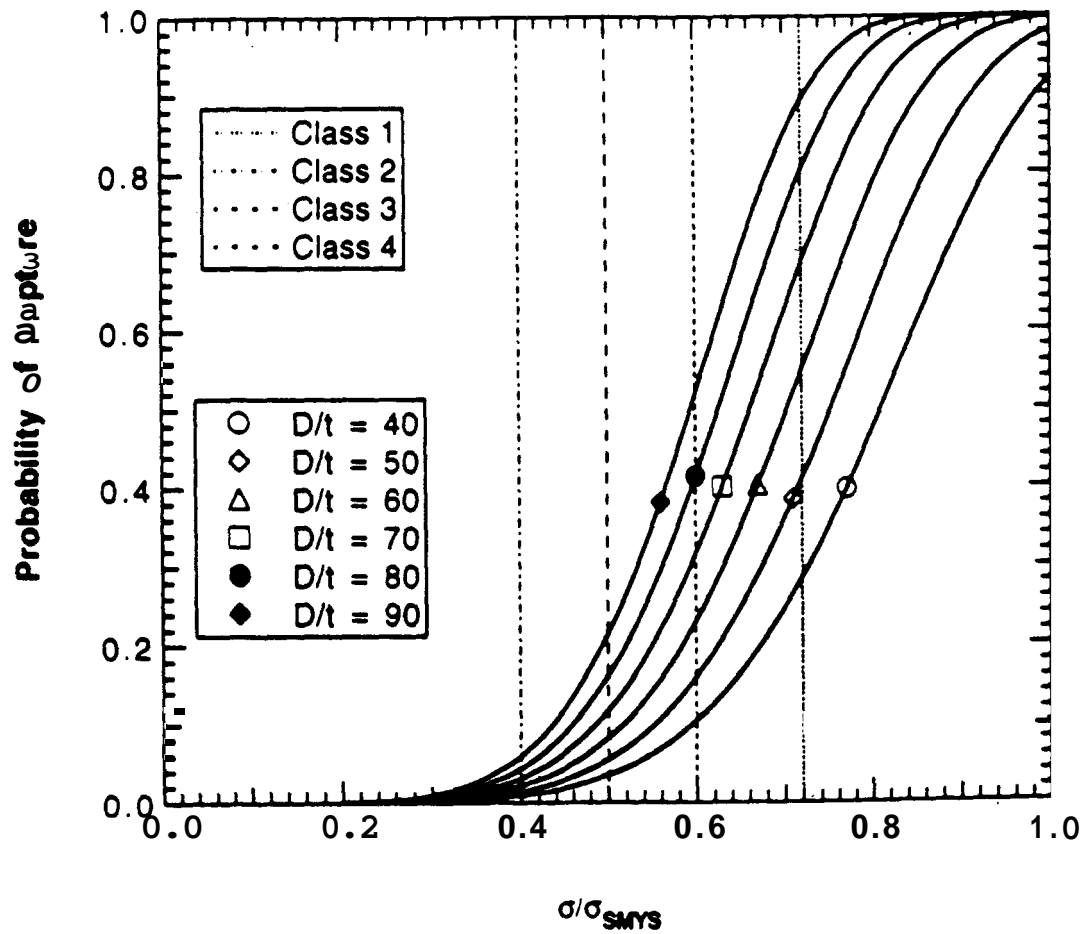


Figure 16. Probability of rupture as a function of the hoop stress for X60 steel pipes having different diameter to thickness ratios D/t . The predictions presented in the figure are specific to the Charpy data set in Table 5 and are not intended to be a prediction for all X60 steel.

point where in Class 1 it is almost certain that dynamic fracture propagation will follow the appearance of a large through-wall crack. However, it should be remembered that these conclusions are based on some problematic materials data in which old X52 is tougher than newer X60 and on the use of only Charpy data to get "S", assuming implicitly no change in constraint with thickness, a questionable assumption at best, but a necessary one to use the data from the literature.

For pipelines (with the Charpy properties in Tables 4 and 5) transporting natural gas, it was found that the leak-before-rupture criterion would likely be satisfied for pipe operating in accordance with CFR ~~Part~~ 192 for Class 3 and 4. However, because the likelihood of third party mechanical damage is considerably less in the latter class locations, and rupture cannot occur in the absence of an initial breach of the pipe wall, together with the fact that transmission pipelines are most often operated at pressures well below the MAOP, it is concluded that there is not an urgent need to make major changes in the currently regulations.

These conclusions must be tempered by the fact that the predictions made herein were based upon estimates of the fracture resistance that were uncertain at best. The assumptions that (1) one can obtain S_c values from Charpy and DWTT results and (2) one can reliably predict DWTT specific fracture energy from Charpy data require yet a third assumption: namely that the specific fracture energy is independent of thickness. These assumptions would at best be fair for X52 steel and poor for more ductile steels such as X60. Consequently, because of the lack of complete and unequivocal line pipe steel material property data, consideration should be given to performing the same analyses with a better measure of the fracture resistance than was available for the present work.

Charpy V-Notch data for X52 and X60 steels suggest an additional problem: that a significant variation in the fracture resistance may exist within a grade of line pipe steel. Hence, sufficient testing must be performed on different steels having the same grade to ensure a statistically meaningful sampling.

The first priority for additional research in this problem area would be the determination of the specific energy gradient, S_c , for X52 and X60 steels with experiments on a suitable range of X52 and X60 steels. Additional topics that would be of value would be:

1. the effects of gases rich in hydrocarbons,
2. removing the conservatism associated with ignoring the potential for crack arrest in the transient stage that precedes dynamic fracture propagation,
3. the use of mechanical crack arresters, and
4. the effect of backfill.